

Mechanism of Zeolite A Nanocrystal Growth from Colloids at Room Temperature

Svetlana Mintova,^{1,3} Norman H. Olson,² Valentin Valtchev,³ Thomas Bein^{1*}

The formation and growth of crystal nuclei of zeolite A from clear solutions at room temperature were studied with low-dose, high-resolution transmission electron microscopy in field emission mode and with in situ dynamic light scattering. Single zeolite A crystals nucleated in amorphous gel particles of 40 to 80 nanometers within 3 days at room temperature. The resulting nanoscale single crystals (10 to 30 nanometers) were embedded in the amorphous gel particles. The gel particles were consumed during further crystal growth at room temperature, forming a colloidal suspension of zeolite A nanocrystals of 40 to 80 nanometers. On heating this suspension at 80°C, solution-mediated transport resulted in additional substantial crystal growth.

Zeolite molecular sieves are crystalline porous solids whose intricate pore and channel systems in the molecular size range of 0.3 to ~3 nm are the basis for their immense importance in catalysis, separations, and ion exchange (1–6). These materials are usually synthesized from aqueous basic aluminosilicate precursor gels under hydrothermal conditions at elevated temperatures (1–3). The complex self-assembly process of the zeolite involves numerous simultaneous and interdependent equilibria and condensation steps. Very little is known about the nucleation step or about the growth process during the initial few hours of the crystallization of even the simplest zeolites, although proposed mechanisms for different systems range from solution-mediated transport to hydrogel transformation processes (2, 4). Because the events in the early stages are of critical importance in determining the course of the subsequent crystallization, a detailed understanding of these phenomena is highly desirable in order to improve structural and morphological control in the synthesis of these important materials.

It is possible to synthesize nanometer-sized zeolites in so-called clear solutions that can serve as model systems for a fundamental understanding of zeolite nucleation and growth processes. Recent scattering studies of such colloidal suspensions, in particular of silicalite [structure type (MFI)], zeolite L (LTL), and zeolite A (LTA), demonstrate the presence of nanoscale, amorphous, aluminosilicate gel agglomerates that are associated with nucleation and conversion into the final zeolite phase [for example, (7–12)]. Different mechanisms have been discussed regarding this process, including assembly of the lattice through (i) soluble small species from solution (2, 13, 14), (ii) aggregation and realignment of preassembled building blocks containing template molecule/aluminosilicate clusters (15–17), and (iii) transformation of the gel phase (2, 8, 17).

We followed the entire process of gel formation, nucleation, and growth of zeolite A in a clear solution model system that started at room temperature (RT) (18–20). High-resolution transmission electron microscopy (HRTEM), performed with reduced electron doses in field emission mode, was used to examine samples of gel particles and zeolite crystals taken at different time intervals. This technique gives a high amount of structural information and minimal interference with the sample. Complementary dynamic light scattering (DLS), powder x-ray diffraction (XRD), and vibrational spectroscopy were performed to complete the emerging picture of the “birth” of a zeolite crystal.

The first observed stage in the synthesis (21) of the clear aluminosilicate solution was the initial mixture containing all reactants except the organic tetramethylammonium (TMA) template. Spherical objects of about equal size with a diameter of 5 to 10 nm were observed in the HRTEM image (Fig. 1A). Dried samples from this solution did not give reflections in the XRD experiment.

After adding the organic template and mixing for 5 min, aggregates in the size range of 40 to 80 nm were formed (Fig. 1B). By adding the TMA hydroxide (TMAOH·5H₂O) to the initial solution, the pH was increased. This results in an increased electrolyte concentration, and it can also cause chemical

reactions (such as condensation of the sol particles); both of these results could cause the aggregation. The XRD pattern of this sample shows the presence of an amorphous phase (Fig. 2A). Further confirmation of the amorphous nature of the gel aggregates at this point was provided by infrared spectroscopy; a band at 467 cm⁻¹ could be assigned to structure-insensitive T-O bending modes of tetrahedral TO₄ units (T = Si or Al) (1). Another T-O mode at 567 cm⁻¹ is related to the presence of the double four and six rings that are part of the structure of zeolite A; this mode is only observed in samples containing crystalline zeolite A, and its intensity increases in relation to the mode at 467 cm⁻¹ during the course of crystallization between 3 and 7

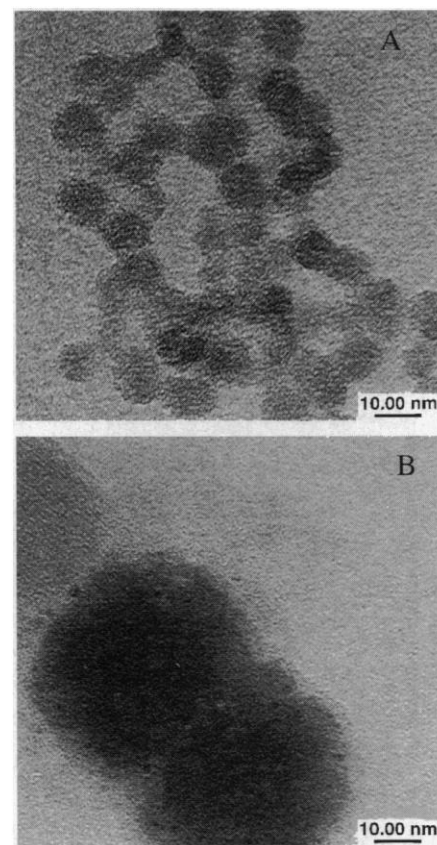


Fig. 1. Gel particles in the initial aluminosilicate solution (A) before adding the organic template and (B) 5 min after adding the organic template for the crystallization of zeolite A. A drop of the washed colloidal suspension was placed on a carbon-coated copper grid and then blotted dry with filter paper. The samples were examined with a Philips CM 200 FEG TEM operated at 200 kV. The grid was scanned at low magnification to search for the crystals. Focusing and astigmatism correction were then performed at the working magnification on an area ~2.5 μm from the area of interest to reduce the amount of beam damage to the specimen. The beam was then automatically translated back to the area of interest immediately before the image was captured by a Gatan 794 multiscan charge-coupled device camera.

¹Department of Chemistry, ²Department of Biology, Purdue University, West Lafayette, IN 47907, USA. ³Central Laboratory of Mineralogy and Crystallography, Bulgarian Academy of Sciences, 92 Rakovski Street, 1000 Sofia, Bulgaria.

*To whom correspondence should be addressed. E-mail: tbein@chem.purdue.edu

REPORTS

days. In situ DLS from unperturbed samples confirmed the size range of the gel-zeolite aggregates (40 to 80 nm); this size range was observed starting at 5 min after mixing during the RT synthesis, which lasted 10 days. However, DLS cannot be used to distinguish between amorphous and crystalline phases.

The crystalline zeolite structure emerged from the gel during the first 3 days. After 3 days at RT, extremely small crystallites of zeolite A, which were only 10 to 30 nm in diameter, were observed embedded in amorphous gel aggregates of ~30 to 60 nm (Fig. 3). The size of these crystals corresponded to only 5-, 9-, 14-, and 30-unit cell dimensions, and lattice fringes that could be assigned to the (200) or (220) planes of the cubic structure of LTA were observed. No distinct zeolite A crystallites were discerned in the TEM after only 2 days at RT. The XRD of the corresponding samples (Fig. 2C) showed the emergence of the crystalline phase of LTA after 3 days with all the expected reflections; the line broadening [of the (622) reflection] was evaluated with the Scherrer formula to yield an average crystallite size of ~57 nm. These data demonstrate that the HRTEM images showing tiny embedded crystallites in gel particles were representative of the entire collective sample.

During the continuation of the RT synthesis, the embedded tiny zeolite A crystallites grew at the expense of the surrounding amorphous gel agglomerates until the latter were completely consumed. On the basis of evidence discussed below, we suggest that this process can occur through solution-mediated transport. The resulting nanoscale zeolite A crystallites that were obtained

after 7 days at RT are shown in Fig. 4. Smooth, fully crystalline particles with a diameter of ~40 to 80 nm were formed (XRD, Fig. 2E). These particles are single crystals with the expected lattice fringes [for example, (220) (Fig. 4, bottom)] of zeolite A, not intergrowths of different lattice orientations; this indicates that each zeolite crystal was generated from one single nucleus in one isolated amorphous precursor gel particle. The crystal size, confirmed in situ in the suspension with DLS and with scanning electron microscopy, is similar to that of the amorphous precursor particles. The crystallized zeolite A was stable in the mother liquor for an extended period of time (at least 60 days) at RT.

To address the issue of solution transport during the zeolite synthesis, we heated a suspension containing fully crystalline nanometer-sized zeolite A (obtained after 10 days at RT) at 80°C for 1 and 2 days. Much larger (between 200 to 400 nm) well-developed crystals of zeolite A were formed under these conditions (Figs. 2F and 5). Although no

amorphous gel phase was present in the suspension, very effective crystal growth was achieved in this system. The total mass of the nanocrystals obtained after 7 days at RT (40 to 80 nm) is very similar to the mass of the large crystals (200 to 400 nm) that were formed after subsequent hydrothermal treatment at 80°C for 1 day (1.6 ± 0.1 weight %). Therefore, the nutrient pool must have been the nanometer-sized zeolite A that formed at RT, thus resembling Ostwald ripening of other sparingly soluble crystals. The remarkable aspect of this observation is that zeolite A can grow through solution transport over large distances. The species involved were presumably the small aluminosilicate ions that are soluble at the high pH of the system (pH = 13.8).

The following mechanism of zeolite crystal growth in this system emerged from our observations (Fig. 6). The aluminosilicate solution contained small particles of ~5 nm

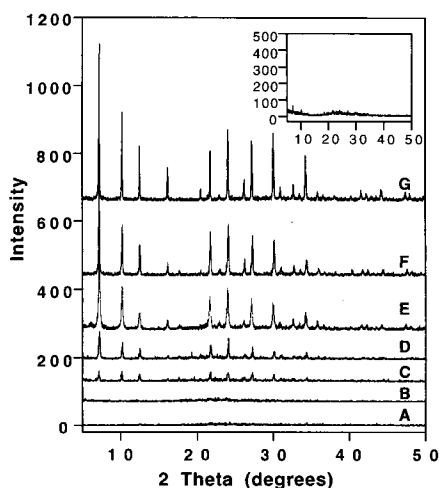


Fig. 2. XRD patterns of the evolution of zeolite A from colloidal suspensions at RT (A) 5 min after mixing precursor solutions; after (B) 1, (C) 3, (D) 4, and (E) 7 days; and (F) after 1 day at 80°C. (G) Commercial zeolite NaA. The inset shows the XRD pattern after 50 hours at RT.

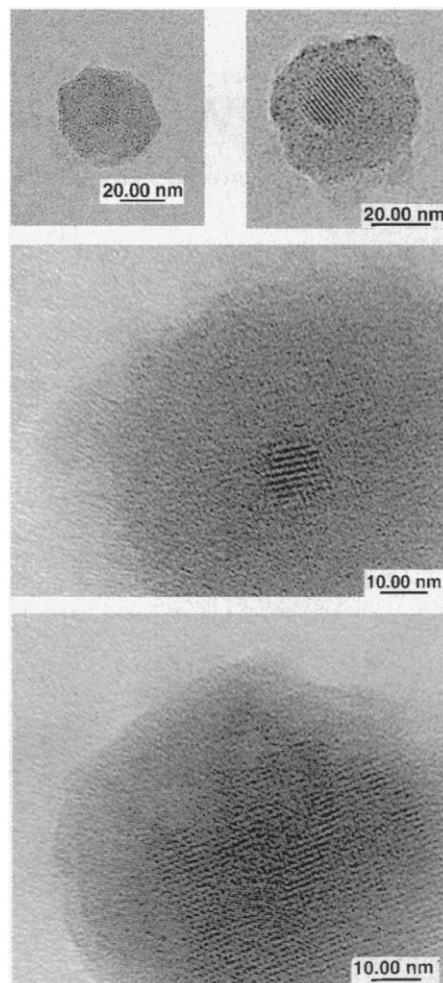


Fig. 3. The "birth" of nanoscale crystallites of zeolite A in four different gel particles, obtained after 3 days of crystallization at RT.

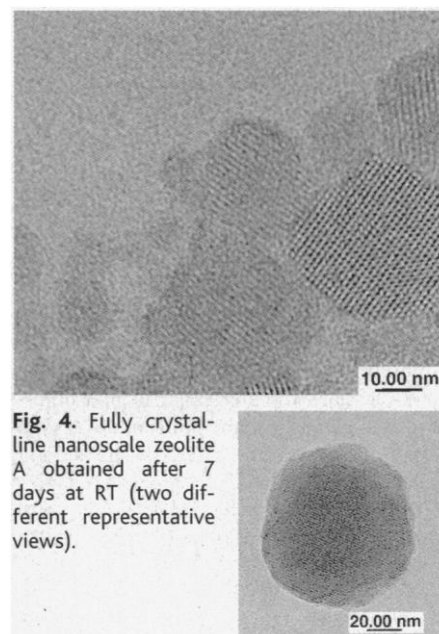


Fig. 4. Fully crystalline nanoscale zeolite A obtained after 7 days at RT (two different representative views).

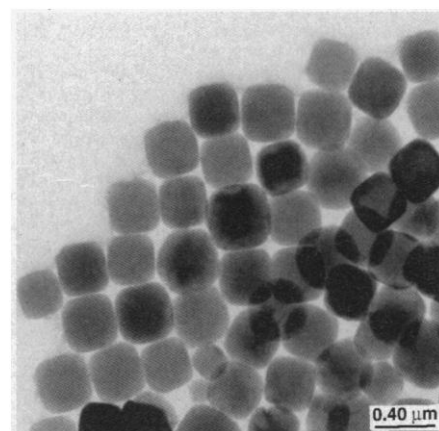


Fig. 5. Zeolite A obtained at 80°C after 1 day of hydrothermal treatment.

REPORTS

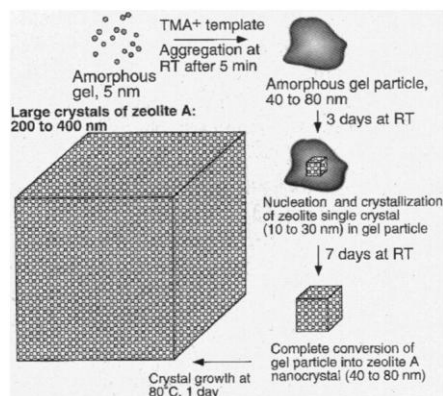


Fig. 6. A schematic representation of the proposed zeolite growth mechanism.

that quickly agglomerated after the addition of the organic template to give 40- to 80-nm amorphous aggregates. Zeolite A was nucleated in these aggregates within 3 days at RT. In the system under study, we observed only one single zeolite crystal per amorphous gel particle; thus, aggregation of several nuclei is clearly not needed to achieve crystallization. We propose that high supersaturation within the gel particles, possibly coupled with preorganization at the interface of the amorphous network with occluded solution, is the driving force for nucleation [see also (14)]. The amorphous gel-zeolite particles maintained their average size over the course of the complete conversion into (more dense) zeolite A, suggesting that mass transfer from solution supplies some of the precursor material. Solution mass transfer must be the dominant mechanism for the substantial crystal growth in the same zeolite A suspension at elevated temperature (no amorphous precursor material was present), so that solution-mediated transport at RT should also be feasible.

References and Notes

1. D. W. Breck, *Zeolite Molecular Sieves* (Wiley, London, 1974).
2. M. E. Davis and R. F. Lobo, *Chem. Mater.* **4**, 756 (1992).
3. H. Kessler, in *Solid-State Supramolecular Chemistry: Two- and Three-Dimensional Inorganic Networks*, vol. 7 of *Comprehensive Supramolecular Chemistry*, G. Alberti and T. Bein, Eds. (Elsevier, Tarrytown, NY, 1996), pp. 425–464.
4. S. L. Burkett and M. E. Davis, *ibid.*, pp. 465–483.
5. W. M. Meier, D. H. Olson, Ch. Baerlocher, *Atlas of Zeolite Structure Types* (Elsevier, London, 1996).
6. S. Feng and T. Bein, *Nature* **368**, 834 (1994); *Science* **265**, 1839 (1994); Y. Yan and T. Bein, *J. Am. Chem. Soc.* **117**, 9990 (1995); S. Mintova *et al.*, *Adv. Mater.* **9**, 585 (1997); G. A. Ozin, *ibid.* **4**, 612 (1992); P. Behrens and G. A. Stucky, in *Solid-State Supramolecular Chemistry: Two- and Three-Dimensional Inorganic Networks*, vol. 7 of *Comprehensive Supramolecular Chemistry*, G. Alberti and T. Bein, Eds. (Elsevier, Tarrytown, NY, 1996), pp. 721–772; T. Bein, *Chem. Mater.* **8**, 1636 (1996).
7. T. A. M. Twomey, M. Mackay, H. P. C. E. Kuipers, R. W. Thompson, *Zeolites* **14**, 162 (1994).

8. M. Tsapatsis, M. Lovallo, M. E. Davis, *Micropor. Mater.* **5**, 381 (1996).
9. A. E. Persson, B. J. Schoeman, J. Sterte, J.-E. Otterstedt, *Zeolites* **14**, 557 (1994); B. J. Schoeman, *ibid.* **18**, 97 (1997); *Micropor. Mesopor. Mater.* **22**, 9 (1998); B. J. Schoeman, J. Sterte, J.-E. Otterstedt, *Zeolites* **14**, 110, (1994); J. Dougherty, L. E. Iton, J. W. White, *ibid.* **15**, 640 (1995).
10. C. Zhu *et al.*, *Chem. Mater.* **10**, 1483 (1998).
11. R. Ravishanker *et al.*, *J. Phys. Chem. B.* **102**, 2633 (1998).
12. L. Gora, K. Streltzyk, R. W. Thompson, G. D. J. Phillips, *Zeolites* **18**, 119 (1997); L. Gora and R. W. Thompson, *ibid.*, p. 132.
13. C. S. Cundy, B. M. Lowe, D. M. Sinclair, *J. Cryst. Growth* **100**, 189 (1990); C. S. Cundy, M. S. Henty, R. J. Plaisted, *Zeolites* **15**, 342 (1995).
14. S. L. Burkett and M. E. Davis, *J. Phys. Chem.* **98**, 4647 (1994).
15. O. Regev, Y. Cohen, E. Kehat, Y. Talmon, *Zeolites* **14**, 314 (1994).
16. R. W. Corkery and B. W. Ninham, *ibid.* **18**, 379 (1997).
17. W. H. Dokter, H. F. van Garderen, T. P. M. Beelen, R. A. van Santen, W. Bras, *Angew. Chem. Int. Ed. Engl.* **34**, 73 (1995).
18. Very few zeolite syntheses have been reported at low temperature [including (TPA)-silicalite-1, which can be obtained within 18 to 24 months below 35°C (16); several beryllophosphates, zincophosphates, and arsenates synthesized at 4° to 100°C (19); and zeolite A, which can be obtained from a RT gel after 30 days (20)].
19. T. E. Gier and G. Stucky, *Nature* **349**, 508 (1991).
20. L. B. Sand, A. Sacco Jr., R. W. Thompson, A. G. Dixon, *Zeolites* **7**, 387 (1987).
21. For the synthesis of zeolite A, clear aluminosilicate

solutions with composition $(0.3 \text{ to } 0.45)\text{Na}_2\text{O}:(4.5 \text{ to } 12)\text{SiO}_2:(0.6 \text{ to } 2)\text{Al}_2\text{O}_3:(9 \text{ to } 14)(\text{TMA})_2\text{O}:(400 \text{ to } 800)\text{H}_2\text{O}$ were prepared and mixed at RT on an orbital shaker (175 rpm) for 1 to 10 days. The composition studied most extensively was $0.3\text{Na}_2\text{O}:\text{11.25SiO}_2:\text{1.8Al}_2\text{O}_3:\text{13.4(TMA)}_2\text{O}:\text{700H}_2\text{O}$. These systems were prepared with a 30% silica sol (containing NaOH to pH = 10) (Aldrich), aluminium isopropoxide $[\text{Al(OiPr)}_3]$ (Aldrich), 97% TMAOH·5H₂O (Aldrich), NaOH (Mallinckrodt, Chesterfield, MO), and filtered doubly distilled H₂O. The gels were prepared from two solutions: Solution I was composed of 2.25 g of 30% silica sol (pH = 10) and 2.0 g of H₂O, and solution II was composed of 0.75 g of Al(OiPr)_3 , 5.00 g of TMAOH·5H₂O, 0.6 g of 1 M NaOH, and 7.0 g of H₂O. To start the zeolite synthesis, we mixed the two precursor solutions under stirring. The solid phase contained in the colloidal suspensions (gel or zeolite particles) was recovered by repeated (three times) cycles of ultracentrifugation at 20,000 rpm for 1 hour, decanting, and ultrasonic redispersion in pure water. The growth of zeolite A was also performed at an elevated temperature (80°C for 1 to 2 days), starting with the colloidal suspension that had reacted for 10 days on the shaker at RT.

22. The authors gratefully acknowledge funding from the U.S. National Research Council (Twinning Program) (T.B. and S.M.) and NSF (T.B.). This work was supported by a NIH biology grant to T. S. Baker (GM 33050), a NSF shared equipment grant (to T.S.B., BIR 9112921), and a grant from the Lucille P. Markey charitable trust to the Purdue Structural Biology Center.

14 October 1998; accepted 11 January 1999

Giant Wormlike Rubber Micelles

You-Yeon Won, H. Ted Davis, Frank S. Bates*

A low molecular weight poly(ethyleneoxide)-poly(butadiene) (PEO-PB) diblock copolymer containing 50 weight percent PEO forms gigantic wormlike micelles at low concentrations (<5 percent by weight) in water. Subsequent generation of free radicals with a conventional water-based redox reaction leads to chemical cross-linking of the PB cores without disruption of the cylindrical morphology, as evidenced by cryotransmission electron microscopy and small-angle neutron scattering experiments. These wormlike rubber micelles exhibit unusual viscoelastic properties in water.

Self-assembly of amphiphilic molecules provides a fundamental mechanism for building complex soft materials. Familiar examples include lipid bilayers, the basic element of cell membranes, soap solutions composed of oil containing micellar globules in an aqueous medium, and pressure-sensitive adhesives formulated with ordered block copolymers. By tailoring the molecular architecture and distribution of chemical functionality, discrete supramolecular objects can be created with prescribed shape, size, and state of order. The physical consequences of minor variations in molecular structure can be dramatic, particularly in the dilute limit where small amounts of amphiphile are added to a

solvent, often water. This report describes a new type of self-assembled object—giant wormlike micelles that can be chemically cross-linked after dispersion in water. These fixed micelles are actually individual macromolecules with molar masses that are more than three orders of magnitude greater than those typical of large conventional synthetic polymers, $\sim 10^5$ to 10^6 g/mol. They have a profound effect on the properties of water at small concentrations and can be directly imaged in vitrified aqueous solution by electron microscopy.

During the past few years we have been experimenting with macromolecular surfactants comprised of poly(ethyleneoxide) (PEO) and various hydrocarbon polymers such as poly(butadiene) (PB) and the saturated analog poly(ethylene) (PEE) (1, 2). Our PEO-PB (I) and PEO-PEE (II) diblock copolymers,

Department of Chemical Engineering and Materials Science, University of Minnesota, Minneapolis, MN 55455, USA.

*To whom correspondence should be addressed.